crystals

Communication

Fabrication of Lettuce-Like ZnO Gas Sensor with Enhanced H_2S Gas Sensitivity

Ziyang Yu [1], Jie Gao [2], Longxiao Xu [1], Tianyu Liu [1], Yueying Liu [1], Xiangyue Wang [3], Hui Suo [1,*] and Chun Zhao [1,*]

1 State Key Laboratory of Integrated Optoelectronics, College of Electronic Science and Engineering, Jilin University, Changchun 130118, China; yuziyang1991@163.com (Z.Y.); xulx18@mails.jlu.edu.cn (L.X.); liuty17@mails.jlu.edu.cn (T.L.); liuyy17@mails.jlu.edu.cn (Y.L.)
2 College of Electronic Science and Engineering, Jilin University, Changchun 130118, China; gao1229jie@163.com
3 College of Chemistry, Jilin University, Changchun 130118, China; xiangyue18@mails.jlu.edu.cn
* Correspondence: suohui@jlu.edu.cn (H.S.); zchun@jlu.edu.cn (C.Z.)

Received: 16 January 2020; Accepted: 17 February 2020; Published: 26 February 2020

Abstract: In this work, a lettuce-like ZnO gas sensor with high sensitivity for H_2S detection was successfully fabricated by a one-step hydrothermal method. Characterization analysis of the phases, crystallinities, morphology, and chemical compositions indicated that lettuce-like ZnO has a lettuce-like microsphere structure composed of wurtzite hexagonal ZnO sheets. A gas sensitivity test of the lettuce-like ZnO showed that the sensor had a high H_2S response (113.04 for 100 ppm H_2S) and H_2S selectivity. The lettuce-like ZnO sensor has fast response characteristics while maintaining high sensitivity, and has a response time as low as 15 seconds and a recovery time of 90 seconds, and the detection limit reaches 1 ppm. The sensitive mechanism of lettuce-like ZnO sensor to H_2S is also discussed.

Keywords: ZnO; microspheres; gas sensors; H_2S; fast response

1. Introduction

Metal oxide semiconductor materials play an important role in the field of gas sensors. However, metal oxide gas sensing materials have the disadvantages of a high operating temperature and high response time, which restricts the application of metal oxide materials in gas sensing. Therefore, the preparation of gas-sensitive materials with both high sensitivity and fast response characteristics is significant for the development and application of sensors. ZnO, as a wide band-gap semiconductor material (Eg = 3.37 eV), has particularly important research significance [1–5].

H_2S, which causes great damage to human health, has long been recognized as an acute neurotoxin. For example: (1) Inhalation of a small amount of H_2S gas can be fatal in a short amount of time; (2) even low concentrations of H_2S can affect the human visual system, respiratory system, and central nervous system [6–8]; (3) based on previous reports, the short-term (10 minutes) and long-term (eight hours) exposure limits for humans in a H_2S atmosphere are 15 ppm and 10 ppm [9], respectively; and (4) at the same time, under aerobic and hot and humid conditions, H_2S sulfur-containing gas will have a strong corrosive effect on various metal pipelines, and may also cause catalyst deactivation, which may cause energy or efficiency loss [10]. In addition, H_2S is an atmospheric pollutant and an important source of acid rain [11]. The development of high-performance H_2S gas sensors has become an urgent need. Currently, H_2S gas can be monitored using chemiresistive sensors made of ZnO [12], α-Fe_2O_3 [13], TiO_2 [14], WO_3 [15], CuO/SnO_2 [16], and β-$AgVO_3$ [17]. Huber and colleagues prepared ZnO nanowires by CVD (Chemical Vapor Deposition) for H_2S detection. The detection limit was as low as 50 ppb [18]. Lin and colleagues prepared a sensor coated with ZnO nanonails. The sensor had a fast response (39 s) and recovery (61 s) to H_2S gas [19].

In this work, we fabricated a lettuce-like ZnO sensor with enhanced H_2S gas sensitivity. We first prepared lettuce-like ZnO nanoparticles by a one-step hydrothermal method, and we performed XRD and SEM characterization of the materials, and determined the phase, crystallographic information, and morphology of lettuce-like ZnO. The lettuce-like ZnO showed a high H_2S response at a low operating temperature. The sensitive materials possessed excellent H_2S selectivity and fast response/recovery. Lettuce-like ZnO materials have a unique morphology of lettuce microspheres, leading to an excellent H_2S adsorption efficiency, which gives the sensor a fast response time. Compared with other works, the lettuce-like ZnO sensor has the advantages of both fast response and high sensitivity. In addition, the sensitive mechanism of lettuce-like ZnO has been discussed.

2. Experiment

All the chemicals used in this study were of analytical grade purchased from Beijing Chemical Works without further purification. The preparation of the lettuce-like ZnO materials is described as follows: Firstly, 0.13 g of glycine, 0.146 g of $Zn(CH_3COO)_2{\cdot}2H_2O$, and 0.13 g of $Na_2SO_4{\cdot}10H_2O$, were added to a mixed solvent of 5 mL of ethanol and 4 mL of deionized water. The mixture was stirred for 5 minutes until all was dissolved. Then, 0.13 g of NaOH was slowly added to the solution with magnetic stirring for 30 minutes, until the solution formed a white gel. The precursor was then transferred to a 20 mL Teflon-lined stainless steel autoclave and heated at 180 °C for 12 hours. After the autoclave was cooled down to room temperature, the precipitates were collected and washed several times with deionized water and ethanol by centrifugation. The dried precipitates were calcined at 400 °C for 2 hours. The products were cured by heating at 200 °C for 1 hour when coated on a ceramic tube for a gas sensitivity test.

The phases, crystallinities, and chemical compositions of the lettuce-like ZnO were examined by means of X-ray diffraction (XRD, Rigaku D/Max 2550, Rigaku, Ltd, Tokyo, Japan) with a Cu Kα radiation line of 0.1506 nm at 40 kV, 200 mA, and by means of a transmission electron microscope (TEM, JEOL JEM-3010, JEOL, Ltd, Tokyo, Japan). Morphology studies were conducted by means of the field emission electron microscopy (FESEM, JEOL, JSM-7500 F, JEOL, Ltd, Tokyo, Japan). The gas-sensitive performance was tested by our laboratory-made gas-sensitive test system, which includes gas-sensitive components, gas cylinders, a Fluke 8846A digital multimeter, a GPD3303S DC power supply, and a computer workstation. The gas response has been defined as S = Ra/Rg. While in an oxidizing atmosphere, the gas response has been defined as S = Rg/Ra. In the formula, Ra and Rg are the electrical resistance of the component in the air and the target gas. The response and recovery time were defined as the time taken to reach 90% of the final stable resistance change value. All gas sensitivity tests were performed at 60% relative humidity.

3. Results and Discussion

The powder XRD pattern of lettuce-like ZnO is shown in Figure 1. The intensity has been shown in a log scale. All diffraction peaks matched the standard peak values of ZnO (JCPDS No.36−1451), which indicates that the ZnO obtained after hydrothermal synthesis and calcination was a wurtzite hexagonal structure ZnO with lattice constants a = b = 3.243 Å and c = 5.195 Å. The thickness of the grains (D) on a certain crystal plane was calculated by the Debye–Scherrer equation [20]: $D = 0.89\lambda/(\beta\cos\theta)$, where λ is the X-ray wavelength (Cu Kα, 0.1506 nm), β is full width at half maxima (FWHM), and θ is the corresponding Bragg diffraction angle. The best response intensity of the XRD pattern of 31.7°, 34.4°, and 36.2° belonged to (100), (002), and (101) planes, and the sizes were calculated to be 46.4 nm, 49.9 nm, and 41.0 nm, respectively.

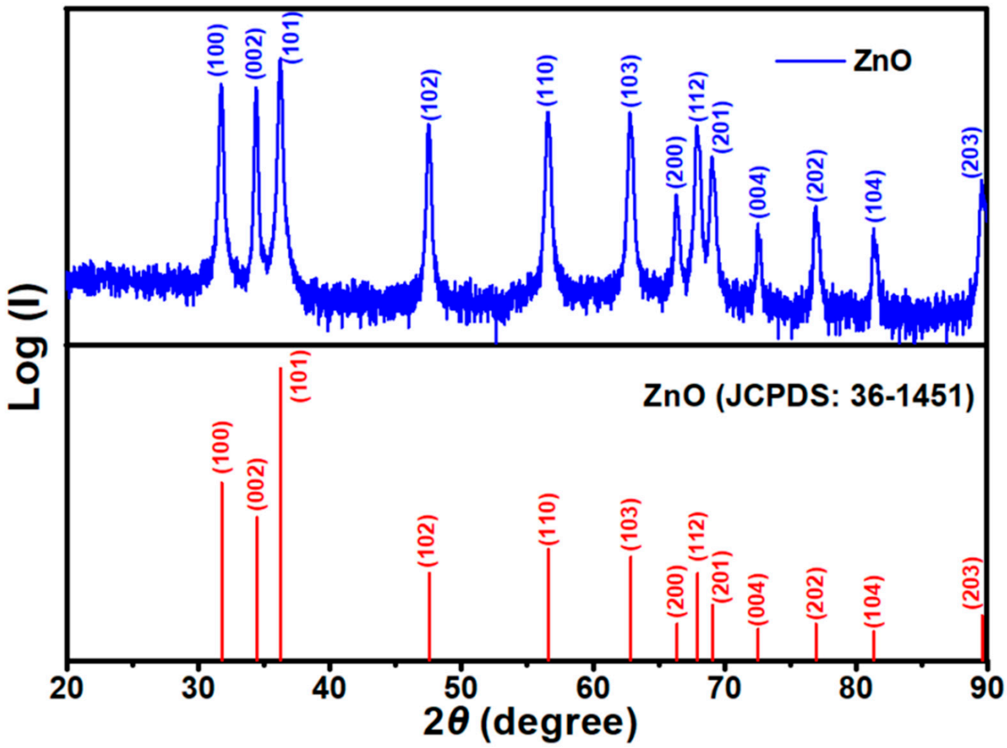

Figure 1. XRD pattern of the as-prepared lettuce-like ZnO.

Figure 2 is the SEM images of the micro-morphology and structure of lettuce-like ZnO. As shown in Figure 2a, after the hydrothermal reaction, the precursor before calcination had no characteristic morphology. Obviously, the precursor did not undergo crystallization during this period. SEM images of lettuce-like ZnO synthesized by hydrothermal and 400 °C calcination are exhibited in Figure 2b–d. The microscopic morphology of ZnO shows a uniform lettuce spherical shape without other morphologies appearing (Figure 2b). The diameter of the lettuce sphere is about 3-4 μm. Every sphere is a ZnO cluster composed of many ZnO sheets, and there are crosses but little overlap between the ZnO sheets (Figure 2c). As shown in Figure 3d, the thickness of the ZnO sheet is about 40–50 nm; this matches the thickness calculated by the previous Debye-Scherrer equation (46.4 nm, 49.9 nm, 41.0 nm). In our other work, some optimizations to control crystallinity have been founded, which are not reported here. The size of ZnO grains will increase with the increasing of the calcination temperature [21], and the morphology will tend to be non-angular spheres due to the overlapping growth of adjacent grains.

The gas sensor's performance was tested for different operating temperatures. Figure 3a shows the gas response of the lettuce-like ZnO to 100 ppm H_2S gas at various operating temperatures from 20 °C to 250 °C. When the temperature is lower than 50 °C, the resistance of lettuce-like ZnO in the air exceeds the range of the tester. Generally, the resistance of semiconductor materials exceeds 1000 Mohm at room temperature, and the resistance of materials can be reduced by increasing the operating temperature. Compared with commercially available ZnO, with the increasing operating temperature, lettuce-like ZnO has a better H_2S sensitivity response at an operating temperature of 150 °C, with a response of 113.04. The operating temperature of lettuce-like ZnO, which reached its maximum sensitivity response, is lower than that of some other researches (250–300 °C) [20,22–26]. This characteristic was attributed to the special morphology of lettuce-like ZnO. Sheet-layered ZnO has a larger specific surface area, so it can better contact the target gas and has more adsorbed oxygen. This process has been proven to reduce the operating temperature of the materials [27]. The selectivity of a lettuce-like ZnO sensor has also been tested. The selectivity of the sensor to 100 ppm of various gases is shown in Figure 3b.

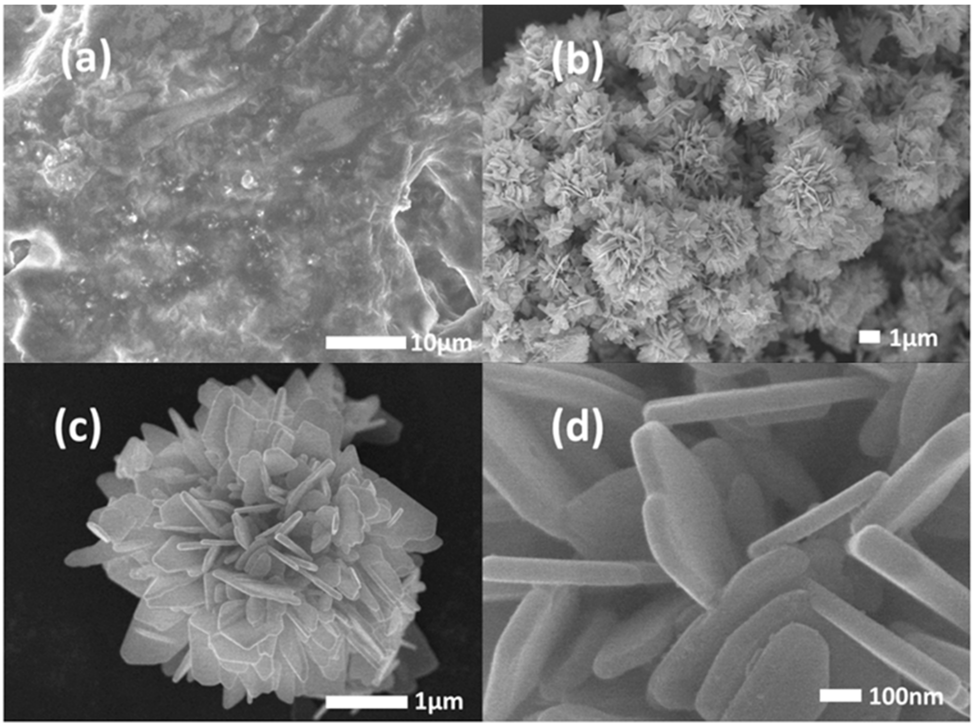

Figure 2. Representative SEM images of (**a**) the ZnO precursor before calcination; (**b**–**d**) the as-prepared lettuce-like ZnO.

The dynamic response cycle of the lettuce-like ZnO sensor using H_2S as the target gas has also been measured and the results are shown in Figure 3c. After the H_2S intake and transpiration for a cycle of five times, the lettuce-like ZnO sensor can still recover the initial resistance, indicating that the sensor has excellent repeatability. The sensor response recovery is equally quick. A single cycle is shown in Figure 3d. Generally, the response time and recovery time of the sensor are the time required for the resistance signal to change to 90% after the intake or transpiration of the gas, respectively [28]. The response time and recovery time of the lettuce-like ZnO sensor to 100 ppm H_2S gas are 15 seconds and 90 seconds, respectively, suggesting that the sensor shows unique response recovery characteristics.

The detection limit of the material has been tested. Figure 3e reveals the dynamic response curve of the lettuce-like ZnO sensor at a concentration range of 1 ppm to 100 ppm H_2S gas at 150 °C. It can be seen that, as the target gas concentration increases, the gas-sensitive response of the sensor increases rapidly. The minimum concentration of H_2S gas that the sensor can detect is around 1 ppm, and the gas response is 1.42 at this time. The sensitivity response to the gas at different concentrations is shown in Figure 3f, and the response of the sensor has a good linearity with the concentration change from 1 ppm to 100 ppm. The long-term stability of the lettuce-like ZnO sensor is shown in Figure 4.

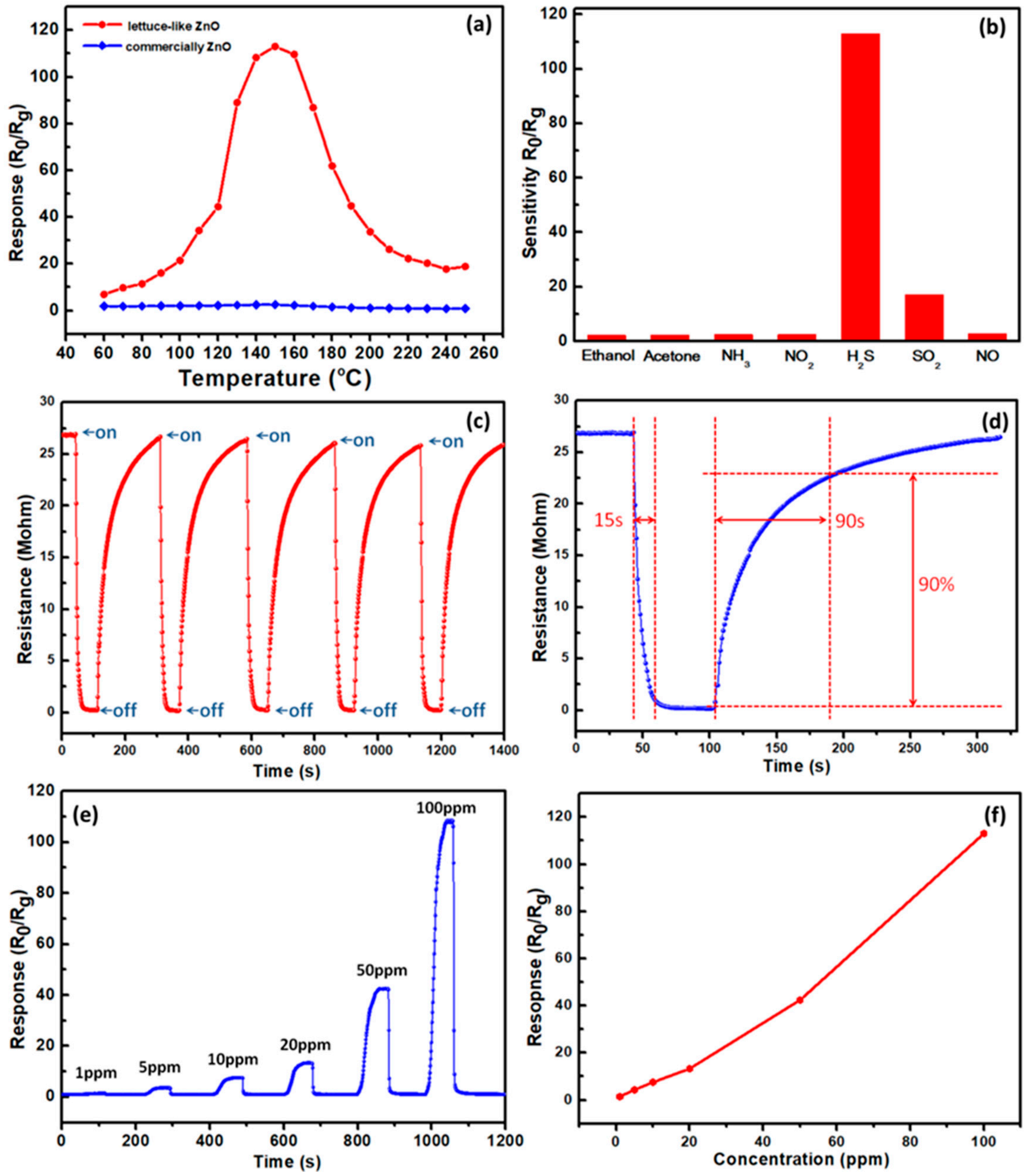

Figure 3. (**a**) Gas sensing response of lettuce-like ZnO sensors and commercial ZnO at different operating temperatures to 100 ppm H_2S, (**b**) the selectivity of lettuce-like ZnO sensors to 100 ppm different gases, (**c**) the repeatability of lettuce-like ZnO sensors at 150 °C to 100 ppm H_2S, (**d**) the response and recovery of lettuce-like ZnO sensors to 100 ppm H_2S, (**e**) the dynamic response of lettuce-like ZnO sensors to 1−100 ppm H_2S at 150 °C, (**f**) the response of lettuce-like ZnO sensors to 1−100 ppm H_2S at 150 °C.

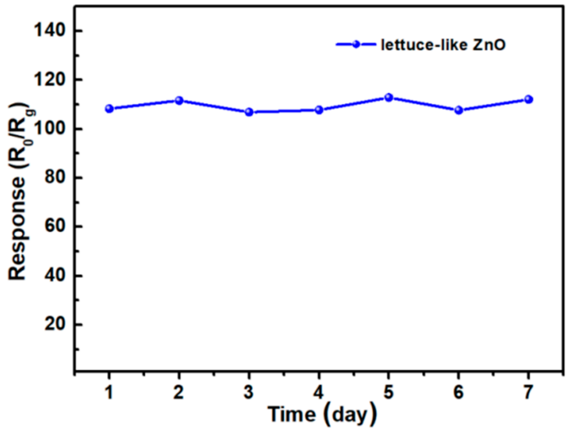

Figure 4. The long-term stability of the lettuce-like ZnO sensor to 100 ppm H_2S.

The mechanism of the lettuce-like ZnO sensors that exhibit enhanced H_2S gas-sensing performance is generally explained as follows: ZnO is a wide band gap n-type semiconductor, suitable for the interpretation of the classic electron depletion model [29,30]. When lettuce-like ZnO is exposed to the air, a chemical adsorption reaction occurs on the surface of the material. Oxygen molecules in the air form adsorption groups such as O^-, O_2^-, and O^{2-} by capturing electrons, which are the carriers of semiconductor material. ZnO being deprived of electrons leads to a larger depletion layer and relatively higher resistance. When the lettuce-like ZnO is exposed to target gas, the adsorption group turns to capture the electrons of H_2S while returning the electrons to the semiconductor material, and the carrier concentration of the material increases, leading to a reduction in the depletion layer and the resistance of the material. At lower temperatures (below 150 °C) [31], the ionic group adsorbed on the surface of the material is mostly O_2^-. However, O^- and O^{2-} are usually chemically adsorbed on the surface by the material at high temperatures (above 150 °C) [32,33].

$$O_2 + e^- \rightarrow O_2^- \quad (1)$$

$$O^{2-} + e- \rightarrow 2O^- \quad (2)$$

$$O^- + e^- \rightarrow O^{2-} \quad (3)$$

The operating temperature of lettuce-like ZnO sensors is about 150 °C, which is a lower temperature compared to the usual 250–300 °C [34]. O_2^- is involved in the H_2S gas-sensitive response. The process is shown in Figure 5. The reaction is:

$$2\ H_2S + 3\ O_2^-\ (ads) \rightarrow 2\ O_2 + 2\ H_2O + 3\ e^- \quad (4)$$

Generally, conventional bulk material ZnO can only have a small part of its surface to undergo gas-sensitive reactions. However, the lettuce-like ZnO has a large specific surface area due to its special lettuce-like morphology. Pores exist in the microspheres formed by sheets, and the surfaces of these pores provide more reaction sites for H_2S, which greatly improves the efficiency of gas-sensitive reactions. This is also the reason why the operating temperature of lettuce-like ZnO material as a gas sensor (150 °C) is lower than that of some other works (250−300 °C). When the working temperature is lower than 150 °C, the oxygen adsorption group participating in the gas-sensitive reaction is O_2^-. Compared with O^- and O^{2-}, the reaction of H_2S and O_2^- is more conducive to occur and proceed [32].

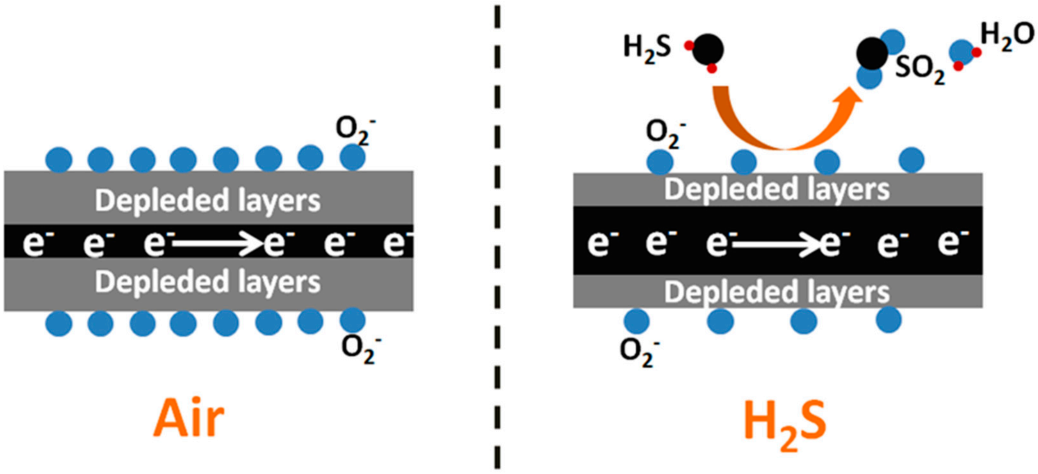

Figure 5. The schematic diagram of the gas-sensing reaction process.

The surface reaction kinetics of different gas molecules are completely different, resulting in different responses to different gases. This is one of the reasons for the unique selectivity of lettuce-like ZnO for H_2S gas. Another possible reason is that the metal oxide on the surface of the material will react with H_2S gas to form a small amount of sulfide ZnS [35].

$$ZnO + H_2S \rightarrow ZnS + H_2O \quad (5)$$

The conductivity of metal sulfides is generally better than that of corresponding metal oxides [36], and its appearance makes the resistance change of lettuce-like ZnO in H_2S more evident.

4. Conclusions

In this work, we synthesized a kind of ZnO with lettuce-like microsphere morphology by the hydrothermal method. The gas-sensitive performance of the lettuce-like ZnO sensor was tested through a gas-sensitive test system assembled in the laboratory. The device has a high response to H_2S gas and excellent selectivity, and has a lower operating temperature (150 °C) and a detection limit as low as 1 ppm due to the special micro-morphology of the material. The lettuce-like ZnO sensor response and recovery time is 15 seconds and 90 seconds, respectively. The sensitivity mechanism of lettuce-like ZnO suggested that by designing and synthesizing a hierarchical structure, a porous morphology, and controlling the crystallinity, the gas-sensitivity performance of semiconductor materials can be effectively improved. This has contributed to the development of high sensitivity and high selectivity sensor materials.

Author Contributions: Conceptualization, Z.Y.; methodology, Z.Y.; investigation, J.G. and L.X.; writing-original draft preparation, Z.Y.; writing-review and editing, Z.Y. All authors have read and agreed to the published version of the manuscript.

Funding: This work is financially supported by the National Natural Science Foundation of China (Grant NOs.61474056 and 51672103).

Conflicts of Interest: The authors declare no conflicts of interest.

References

1. Wagner, T.; Haffer, S.; Weinberger, C.; Klaus, D.; Tiemann, M. Mesporous materials as gas sensors. *Chem. Soc. Rev.* **2013**, *42*, 4036–4053. [CrossRef]
2. Geng, B.; Liu, J.; Wang, C. Multi-layer ZnO architectures: Polymer induced synthesis and their application as gas sensors. *Sens. Actuators B* **2010**, *150*, 742–748. [CrossRef]

3. He, Y.; Zhang, W.; Zhang, S.; Kang, X.; Peng, W.; Xu, Y. Study of the photoconductive ZnO UV detector based on the electrically floated nanowire array. *Sens. Actuators A* **2012**, *181*, 6–12. [CrossRef]
4. Liu, B.; Zeng, H. Hydrothermal synthesis of ZnO nanorods in the diameter regime of 50nm. *J. Am. Chem. Soc.* **2003**, *125*, 4430–4431. [CrossRef] [PubMed]
5. Dhahri, R.; Hjiri, M.; ElMir, L.; Alamri, H.; Bonavita, A.; Iannazzo, D.; Leonardi, S.G.; Neri, G. CO sensing characteristics of In-doped ZnO semiconductor nanoparticles. *J. Sci. Adv. Mater. Devices* **2017**, *2*, 34–40. [CrossRef]
6. Shukla, G.; Bhatnagar, M. H_2S gas sensor based on Cu doped SnO_2 nanostructure. *J. Mater. Sci. Eng. A* **2014**, *4*, 99–104.
7. Katti, V.; Debnath, A.; Muthe, K.; Kaur, M.; Dua, A.; Gadkari, S.; Gupta, S.; Sahni, V. Mechanism of drifts in H_2S sensing properties of SnO_2:CuO composite thin film sensors prepared by thermal evaporation. *Sens. Actuators B* **2003**, *96*, 245–252. [CrossRef]
8. Glass, D.C. A revive of the hellth effect of offs of hydrogen sulphide exposure. *Ann. Occupypatial Hyg.* **1990**, *34*, 323–327.
9. Lia, Y.; Deng, D.; Xing, X.; Chen, N.; Liu, X.; Xiao, X.; Wang, Y. A high performance methanol gas sensor based on palladium-platinum-In_2O_3 composited nanocrystalline SnO_2. *Sens. Actuators B* **2016**, *237*, 133–141. [CrossRef]
10. Guo, K.; Wen, J.; Hao, Y. Optimal Packing of a Rotating Packed Bed for H_2S Removal. *Environ. Sci. Technol.* **2014**, *48*, 6844–6849. [CrossRef]
11. Guo, Z.; Chen, G.; Zeng, G.; Liu, L.; Zhang, C. Metal oxides and metal salt nanos-tructures for hydrogen sulfide sensing: Mechanism and sensing performance. *RSC Adv.* **2015**, *5*, 54793–54805. [CrossRef]
12. Liao, L.; Lu, H.; Li, J.; He, H.; Wang, D.; Fu, D.; Liu, C. Size dependence of gas sensitivity of ZnO nanorods. *J. Phys. Chem. C* **2007**, *111*, 1900–1903. [CrossRef]
13. Sun, Z.; Yuan, H.; Liu, Z.; Han, B.; Zhang, X. A highly efficient chemical sensor material for H_2S: A-Fe_2O_3 nanotubes fabricated using carbon nanotube templates. *Adv. Mater.* **2005**, *17*, 2993–2997. [CrossRef]
14. Liu, T.; Xu, L.; Wang, X.; Li, Q.; Cui, Q.; Suo, H.; Zhao, C. A Simple Dip-Coating Method of SnO_2-NiO Composite Thin Film on a Ceramic Tube Substrate for Methanol Sensing. *Crystals* **2019**, *9*, 621. [CrossRef]
15. Rout, C.; Hegde, M.; Rao, C. H_2S sensors based on tungsten oxide nanostructures. *Sens. Actuators B* **2008**, *128*, 488–493. [CrossRef]
16. Liu, J.; Huang, X.; Ye, G.; Liu, W.; Jiao, Z.; Ghao, W.; Zhou, Z.; Yu, Z. H_2S detection sensing characteristic of CuO/SnO_2 sensor. *Sensors* **2003**, *3*, 110–118. [CrossRef]
17. Mai, L.; Xu, L.; Gao, Q.; Han, C.; Hu, B.; Pi, Y. Single β-$AgVO_3$ nanowire H_2S sensor. *Nano Lett.* **2010**, *10*, 2604–2608. [CrossRef]
18. Huber, F.; Riegert, S.; Madel, M.; Thonke, K. H_2S sensing in the ppb regime with zinc oxide nanowires. *Sens. Actuators B* **2017**, *239*, 358–363. [CrossRef]
19. Lin, J.; Chen, Z.; He, X.; Xie, W. Detection of H_2S at Room Temperature Using ZnO Sensors Based on Hall Effect. *Int. J. Electrochem. Sci.* **2017**, *12*, 6465–6476. [CrossRef]
20. Li, S.; Zhang, L.; Zhu, M.; Ji, G.; Zhao, L.; Yin, J.; Bie, L. Acetone sensing of ZnO nanosheets synthesized using room-temperature precipitation. *Sens. Actuators B* **2017**, *249*, 611–623. [CrossRef]
21. Zhang, L.; Zhao, J.; Lu, H.; Li, L.; Zheng, J.; Li, H.; Zhu, Z. Facile synthesis and ultrahigh ethanol response of hierarchically porous ZnO nanosheets. *Sens. Actuators B* **2012**, *161*, 209–215. [CrossRef]
22. Wang, X.; Zhang, S.; Shao, M.; Huang, J.; Deng, X.; Hou, P.; Xu, X. Fabrication of ZnO/$ZnFe_2O_4$ hollow nanocages through metal organic Frameworks route with enhanced gas sensing properties. *Sens. Actuators B* **2017**, *251*, 27–33. [CrossRef]
23. Kwon, Y.; Kang, S.; Mirzaei, A.; Choi, M.; Bang, J.; Kim, S.; Kim, H. Enhancement of gas sensing properties by the functionalization of ZnO-branched SnO_2 nanowires with Cr_2O_3 nanoparticles. *Sens. Actuators B* **2017**, *249*, 656–666. [CrossRef]
24. Su, X.; Duan, G.; Xu, Z.; Zhou, F.; Cai, W. Structure and thickness-dependent gas sensing responses to NO_2 under UV irradiation for the multilayered ZnO micro/nanostructured porous thin films. *J. Colloid Interface Sci.* **2017**, *503*, 150–158. [CrossRef] [PubMed]
25. Das, M.; Sarkar, D. One-pot synthesis of zinc oxide-polyaniline nanocomposite for fabrication of efficient room temperature ammonia gas sensor. *Ceram. Int.* **2017**, *43*, 11123–11131. [CrossRef]

26. Li, X.; Wang, J.; Xie, D.; X, J.; Xia, Y.; Xiang, L. Enhanced p-type NO_2-sensing properties of ZnO nanowires utilizing CNTs electrode. *Mater. Lett.* **2017**, *206*, 18–21. [CrossRef]
27. Wang, H.; Zhou, L.; Liu, Y.; Liu, F.; Liang, X.; Liu, F.; Gao, Y.; Yan, X.; Lu, G. UV-activated ultrasensitive and fast reversible ppb NO_2 sensing based on ZnO nanorod modified by constructing interfacial electric field with In_2O_3 nanoparticles. *Sens. Actuators B* **2020**, *305*, 127498. [CrossRef]
28. Liu, Y.; Liu, F.; Bai, J.; Liu, T.; Yu, Z.; Dai, M. Direct growth of NiO films on Al_2O_3 ceramics by electrochemical deposition and its excellent H_2S sensing properties. *Sens. Actuators B* **2019**, *296*, 126619. [CrossRef]
29. Miller, D.; Akbar, S.; Morris, P. Nanoscale metal oxide-based heterojunctions for gas sensing: A review. *Sens. Actuators B* **2014**, *204*, 250–272. [CrossRef]
30. Yu, J.; Ippolito, S.; Wlodarski, W.; Strano, M.; Kalantarzadeh, K. Nanorod based schottky contact gas sensors in reversed bias condition. *Nanotechnology* **2010**, *2126*, 265502. [CrossRef]
31. Chang, S. Oxygen chemisorption on tin oxide: Correlation between electrical conductivity and EPR measurements. *J. Vac. Sci. Technol.* **1980**, *144*, 366–369. [CrossRef]
32. Lupan, O.; Ursaki, V.V.; Chai, G.; Chow, L.; Emelchenko, G.A.; Tiginyanu, I.M.; Gruzintsev, A.N.; Redkin, A.N. Selective hydrogen gas nanosensor using individual ZnO nanowire with fast response at room temperature. *Sens. Actuators B* **2010**, *17*, 56–66. [CrossRef]
33. Yamazoe, N.; Fuchigami, J.; Kishikawa, M.; Seiyama, T. Interactions of Tin Oxide Surface With O_2, H_2O and H_2. *Surf. Sci.* **1979**, *86*, 335–344. [CrossRef]
34. Kohl, D. The role of noble metals in the chemistry of solid-state gas sensors. *Sens. Actuators B* **1990**, *1*, 158–165. [CrossRef]
35. Huang, H.; Xu, P.; Zheng, D.; Chen, C.; Li, X. Sulfuration–desulfuration reaction sensing effect of intrinsic ZnO nanowires for high-performance H_2S detection. *J. Mater. Chem. A* **2015**, *3*, 6330–6339. [CrossRef]
36. Luo, W.; Deng, J.; Fu, Q.; Zhou, D.; Hu, Y.; Gong, S.; Zheng, Z. Nanocrystalline SnO_2 film prepared by the aqueous sol–gel method and its application as sensing films of the resistance and SAW H_2S sensor. *Sens. Actuators B* **2015**, *217*, 119–128. [CrossRef]